The Individuality of Relatively Permanent Pigmented or Vascular Skin Marks (RPPVSM) in Independently and Uniformly Distributed Patterns

[1]**Arfika Nurhudatiana**, *Student Member*, *IEEE*, [*1]**Adams Wai-Kin Kong**, *Member*, *IEEE*, [2]**Keyan Matinpour**, [2]**Deborah Chon**, [2]**Lisa Altieri**, [3]**Siu-Yeung Cho**, *Member*, *IEEE*, and [2]**Noah Craft**

[1]Forensics and Security Laboratory, School of Computer Engineering, Nanyang Technological University, Block N4, Nanyang Avenue, Singapore, 639798; [2]Los Angeles Biomedical Research Institute at Harbor-UCLA Medical Center, 1124 West Carson St. HH-207, Torrance, CA 90502 USA; [3]Electrical and Electronic Engineering, Division of Engineering, University of Nottingham Ningbo China, 199 Taikang East Road, Ningbo, China, 315100.

Abstract **—** With recent advances in multimedia technology, the involvement of digital images/videos in crimes has been increasing significantly. Identification of individuals in these images/videos can be challenging. For example, in cases of child sexual abuse, child pornography, and masked gunmen, the faces of criminals or victims are often hidden or covered and only some body parts (e.g., back, thigh, and arm) can be observed from the digital evidence. Although tattoos and scars can be used for identification in some cases, they are neither universal nor unique. We propose a group of skin marks named Relatively Permanent Pigmented or Vascular Skin Marks (RPPVSM) as a biometric trait for forensic identification. To support the scientific underpinnings of using RPPVSM patterns as a novel biometric trait, the individuality was studied. RPPVSM on the backs of 269 male subjects were examined. We found that RPPVSM in middle to low density patterns tend to form an independent and uniform distribution, while RPPVSM in high density patterns tend to form clusters. We present in this paper an individuality model for the independently and uniformly distributed RPPVSM patterns. When compared to the empirical results, this model fits the empirical distribution very well. Finally, the predicted error rates for verification and identification are reported.

Index Terms **—** Skin marks, forensics, individuality, probability of random correspondence, statistics, predicted error rates

[*] Correspondence author: Tel: (65) 6513 8041. E-mail: adamskong@ntu.edu.sg.

I. INTRODUCTION

With recent advances in internet and multimedia technology, the involvement of digital images or videos in crimes has been increasing significantly. In cases of child sexual abuse, child pornography, masked gunmen, and violent protesters (e.g., the London [1] and the Rome [2] riots in 2011), evidence for identifying criminals or victims are often in the form of digital images or videos. Identifying individuals from this digital evidence can be very challenging because the criminals are usually careful to hide or cover their faces. According to Bureau of Justice Statistics report in 2006, the prosecution rate of child sex exploitation offenders was very low, largely due to inadmissible or weak evidence [3]. Child sex exploitation has become a very serious problem worldwide. The U.S. Customs Service estimated that around 100,000 websites were involved with child pornography [4]. In Canada alone, about 30,000 cases of child pornography were reported between 2002 and 2008 [5].

Although in the evidence images/videos of the above cases the faces of the criminals or victims are often not visible, other body parts can be visible. In child sexual exploitation offenses (e.g., child pornography), close-up views of the back, chest, or thighs are often present. The arms of masked gunmen or violent protesters are often visible since they often wear short sleeve shirts. Although tattoos and scars [6]-[8] can be used for identification in these cases, they are not universal. Underage children or adults in certain professions (e.g., school teachers and law enforcement officers) usually do not have tattoos. In addition, tattoos are forbidden by certain religions. Tattoos are also not unique since the same tattoo pattern can be found in many people as in the case of gang tattoos (e.g., Harley-Davidson gang tattoo). As a solution to this matter, body vein patterns were recently introduced as a biometric trait [9]. Body vein patterns are universal since everybody has blood vessels. However, the visibility depends on some physiological factors such as the thickness of subcutaneous fat layer in the skin and pigmentation level. Since skin marks are located at the surface of the skin, they are more easily observable than the blood vessels. Thus, they have more potential to be applied in the above scenarios.

Skin marks are used as additional means of distinctiveness in face recognition or as an alternative identification feature when face recognition fails [10]-[15]. In contrast to that, we propose in this paper relatively permanent pigmented or vascular skin marks (RPPVSM), which are applicable not

only on the face, but almost any part of human body. This concept originated during a criminal prosecution in the U.S. [16] where two co-authors (Kong and Craft) served as expert witnesses. In this case, a criminal sexually offended seven minors. Craft, who is a board-certified dermatologist, manually identified the RPPVSM in the evidence photos and on the skin of the suspect in custody and presented the results of his visual examination and comparisons to the jury during the trial. However, some aspects of the methods were challenged due to lack of previous scientific study on this subject [17]. One challenge that arose during the Daubert hearing preceding the trial was about the individuality or uniqueness of RPPVSM patterns. This paper investigates some of the concerns raised during this legal process.

The contributions of this paper include: 1) analyzing spatial distribution statistics of RPPVSM, 2) developing an individuality model for independently and uniformly distributed RPPVSM patterns, 3) developing a RPPVSM matching algorithm, 4) empirically validating the model, and 5) estimating potential error rates for verification and identification. We collected images from 269 subjects for this study. Our previous study [18] reported general statistics and spatial distribution statistics of RPPVSM in a small database containing images from 144 subjects. It did not provide any statistical model, matching algorithm, and result for individuality study, which are the foci of this paper.

The remainder of this paper is organized as follows: in section II, different types of RPPVSM are presented and their medical properties are given. In section III, spatial distribution statistics of RPPVSM are reported. In section IV, an individuality model for independently and uniformly distributed RPPVSM patterns is proposed. In section V, a RPPVSM matching method is presented. In section VI, experimental results are reported. In section VII, the predicted error rates for verification and identification are offered. In section VIII, discussion and future work are presented. Finally, in section IX, conclusion is given.

II. RELATIVELY PERMANENT PIGMENTED OR VASCULAR SKIN MARKS (RPPVSM)

Several types of skin marks were investigated in this study. Some skin marks change rapidly while some others tend to be stable. Skin marks caused by inflammatory conditions (e.g., eczema and psoriasis), skin trauma, skin allergy, or insect bites have a transient nature while skin marks like nevi,

lentigines (lentigos), cherry hemangiomas, and seborrheic keratoses (see Fig. 1) are stable over time (six months or longer). These four types of skin marks are also common. 98.90% of the subjects in our study have at least one of them on their backs. Since these skin marks occur as a result of increased pigmentation (e.g., nevi and lentigos) or vascular proliferation (e.g., cherry hemangiomas), we named this class of marks "Relatively Permanent Pigmented or Vascular Skin Marks", abbreviated as RPPVSM. The term "relatively permanent" is used because in some rare cases (e.g., halo nevi) some skin marks can appear or disappear over a period of many years [19]-[20].

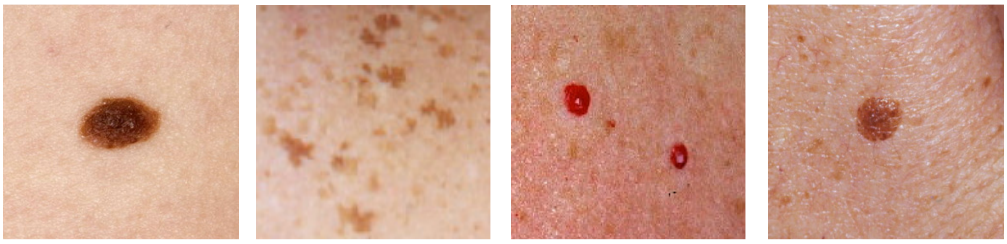

(a) (b) (c) (d)

Fig. 1. Clinical appearance of different types of RPPVSM: (a) nevi, (b) lentigines, (c) cherry hemangiomas, and (d) seborrheic keratoses.

Nevi (melanocytic nevi), commonly known as moles, are sharply-circumscribed and chronic lesions of the skin. They are typically oval or round in shape and their color ranges from skin-colored or brown to black. Nevi occur when melanocytes, which are pigment-producing cells that color the skin, hair, and eye, do not uniformly spread throughout the skin but instead grow in clusters. Most melanocytic nevi are acquired although some are congenital. The acquired melanocytic nevi develop during childhood and adolescence and become stable in middle age [21]. The number of nevi in a person depends on genetic factors and sun exposure [22].

Lentigines are flat pigmented spots on the skin. They can be irregular in shape and their color ranges from skin-colored to tan to brown to black. Lentigines occur as a result of hyperplasia of melanocytes (i.e., an increase in the number of melanocytes) which is linear in its spread [23]. This means that the process is restricted to the cell layer directly above the basement membrane of the epidermis where melanocytes normally reside. This makes lentigines different from nevi as lentigines do not form nests of multi-layered or clustered melanocytes found in nevi. Sometimes lentigines are mistaken as freckles (ephelides). Different from lentigines, freckles have relatively normal number of melanocytes, but an increased amount of melanin. Freckles were not included in RPPVSM because

they intensify and fade with sunlight exposure whereas lentigines are stable regardless of the amount of sunlight exposure [23].

Cherry hemangiomas or cherry angiomas are bright red papules on the skin containing an abnormal proliferation of blood vessels. They are the most common type of angiomas, which are benign cell growths derived from cells of the vascular or lymphatic vessel walls (epithelium) or from cells of the tissues surrounding these vessels. They occur as clusters of tiny capillaries at the surface of the skin, forming small round domes (papules) that are bright red or purple in color. Once the lesions appear, they are relatively permanent and stable over months to years. Cherry hemangiomas are generally associated with aging since many people develop them in the third or fourth decades of their life [24].

Seborrheic keratoses are formed due to proliferations of keratinocytes, the predominant cell type in the epidermis. They can be recognized from their oval, slightly raised and 'stuck-on' appearance. Their development is also associated with aging since the frequency appears to increase with age. Seborrheic keratoses tend to be permanent with a varying degree of pigmentation. In pigmented seborrheic keratoses, the lesions also contain proliferations of melanocytes since the proliferating keratinocytes trigger the activation of neighboring melanocytes [24].

III. SPATIAL DISTRIBUTION STATISTICS OF RPPVSM

RPPVSM on skin can be treated as a point pattern, which is similar to the minutiae on a fingerprint. Therefore, our study refers to the existing fingerprint studies. Fingerprint studies show that: 1) minutiae tend to over disperse when observed on a small scale, but tend to form clusters when observed on a large scale [25]-[27], and 2) minutiae orientations are not independent of minutiae locations [28]-[29]. These properties make modeling the individuality of fingerprint difficult. About twenty fingerprint individuality models have been proposed to date [28]-[36]. From these studies, it can be seen that when accurate assumptions on minutiae properties were employed, the model estimations were close to the empirical results. Thus, we study the spatial distribution statistics of RPPVSM before modeling their individuality.

A common starting point for analyzing spatial point pattern distribution is the test of Complete Spatial Randomness (CSR) hypothesis [37]-[39]. The hypothesis states that: 1) the number of points in any planar region A with area $|A|$ follows a Poisson distribution with mean $\lambda|A|$, where the constant λ is the *intensity*[1] or average number of points per unit area, and 2) given n points in the region A, they are independent random samples from a uniform distribution. This indicates that a point pattern which qualifies the CSR hypothesis corresponds to a homogeneous Poisson distribution, whose random variables are independently and uniformly distributed. Two alternative hypotheses against the null CSR hypothesis are clustering and regular tendencies. In clustered patterns, points tend to locate near others, while in regular patterns points tend to spread far from each other.

Two classical methods for performing the CSR test are the quadrat counts method and the distance method [37]-[40]. The quadrat counts method divides a spatial pattern into quadrats (sub-regions) of equal sizes and computes the number of points in each quadrat. The distance method enumerates all inter-point distances and searches for the shortest distance in order to determine the nearest-neighbor distance for each point. Since the number of RPPVSM in a pattern in our back torso image database reaches over 350, it is more efficient to perform a large scale observation via the quadrat counts method than the distance method. Furthermore, it was shown in [40] that variance-to-mean ratio and Steven's tests, which are types of the quadrat counts method, performed well in the detection of regular, random, and aggregated patterns.

The quadrat counts method divides a domain D into k non-overlapping quadrats $A_1, A_2, \ldots, A_k$ with equal size such that $A_1 \cup A_2 \cup \ldots \cup A_k = D$. Let the number of points in quadrat i be n_i and the total number of points in D be n. The expected number of points in any quadrat under the CSR hypothesis is $\overline{n} = n/k$. Two criteria must be fulfilled to obtain reliable test results — the expected number per quadrat $\overline{n}$ must be greater than 1, and the total number of quadrats k must be greater than 6 [38]-[39]. The acceptance or rejection of a CSR hypothesis is based on the standard Pearson chi-square statistic with (k–1) degrees of freedom given by

[1] The term *intensity* is used to describe average number of points per unit area (density) in the CSR hypothesis.

$$\chi^2 = \sum_{i=1}^{k} \frac{(n_i - \overline{n})^2}{\overline{n}}. \quad (1)$$

This chi-square statistic is also called a variance-to-mean ratio test statistic or the index of dispersion.

A. Database

Our RPPVSM database consists of three sets of back torso images from male Caucasians, Latinos, and Asians. The first set of images was collected in Los Angeles using a Nikon D80 camera (max. resolution of 3872x2592 pixels). It contained mostly Caucasian and Latino subjects. The other two sets of images were collected in Singapore using two cameras — a Nikon D70s camera (max. resolution of 3008x2000 pixels) and a Canon EOS 500D camera (max. resolution of 4752x3168 pixels). These two sets of images contained mostly Asian subjects, which included Chinese, Malay, and Indian ethnic groups. The resolution of all images was 300 dpi. The second and third sets of images were taken in two different sessions with an interval of one week. However, due to limited availability of volunteers, the first set of images was mostly taken in a single session only. The volunteers were seated or standing at a distance between 1 and 1.5 meters from the camera, so the scale was similar for all images. Note that in forensic scenarios, evidence images are usually marked by experts. However, images of inmates or suspects collected in a controlled environment can be handled by automatic algorithms and therefore there is no scale problem.

RPPVSM can be identified on almost every part of the human body. We used back torso because it is the largest flat area on the body where a large number of RPPVSM can be identified. After excluding subjects with large tattoos in their backs, 269 different subjects were used in this statistical study. This is significantly larger than the database used in our previous study which included only 144 subjects [18]. The RPPVSM were manually identified by a medical researcher trained in dermatology and the results were verified by a board-certified dermatologist who testified in the previously mentioned legal case. Fig. 2 shows a raw image of a Caucasian's back with the identified RPPVSM.

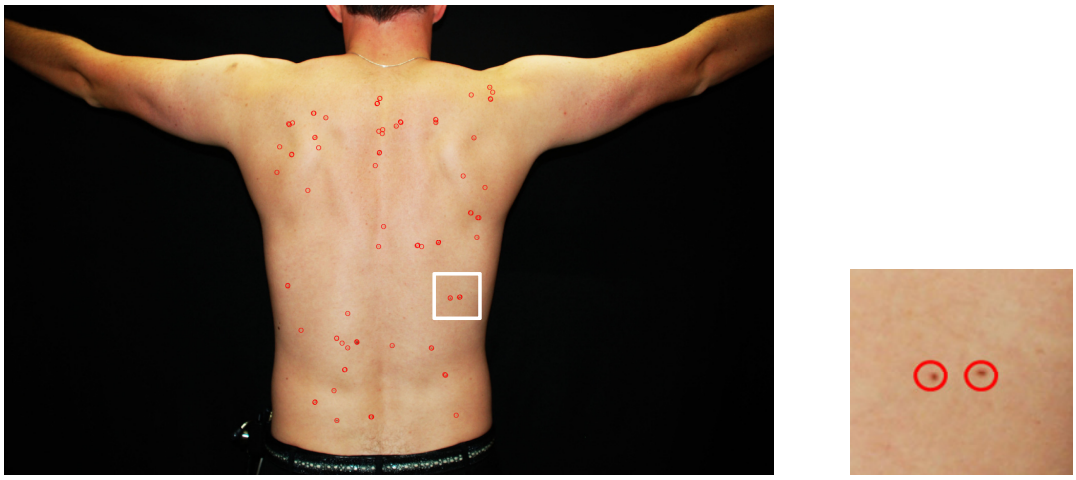

(a) (b)

Fig. 2. A RPPVSM pattern on the back of a Caucasian male; (a) the raw image; circles indicate RPPVSM identified by a researcher trained in dermatology, (b) the enlarged version of the small rectangular box in (a) to show the detected RPPVSM.

B. CSR Test Results and Discussion

Before performing the quadrat counts method, all images were normalized to the smallest maximum resolution (3008x2000 pixels). We used three different quadrat sizes, 3x2, 4x3, and 5x4 to prevent a specific quadrat size from influencing the CSR test results. The minimum quadrat size was set to 3x2 since back has a rectangular shape. Setting the minimum expected number of RPPVSM in each quadrat to 1, the minimum numbers of RPPVSM required for quadrat sizes of 3x2, 4x3, and 5x4 were 6, 12, and 20 respectively. For each quadrat's size, the window size of quadrats in pixel varied depending on the actual size of the back. For example, the width of a slim subject's back is likely to be smaller than the width of a fat subject's back. Similarly, the height of a tall subject's back is likely to be larger than the height of a short subject's back. To accept or reject the CSR hypothesis, we applied a two-tailed test with a 90% confidence interval. If the *p*-value was less than 0.05, the pattern was regarded as clustered; while if the *p*-value was greater than 0.95, the pattern was regarded as regular.

The overall CSR test results grouped by number of RPPVSM are given in Table I. Patterns with 6 to 11 RPPVSM were tested with quadrat size of 3x2 only, and patterns with 12 to 19 RPPVSM were tested with quadrat sizes of 3x2 and 4x3. Patterns which passed the tests with both quadrat sizes were regarded as CSR patterns. The rest of the patterns were tested with the three different quadrat sizes and the final results were determined via majority voting. As seen in Table I, the number of patterns

which qualified the CSR test decreases as the number of RPPVSM increases. A drastic decrement is apparent when the number of RPPVSM is 50 or more. From 161 patterns with 6 to 49 RPPVSM, 124 patterns qualified the CSR hypothesis. However, from 61 patterns with 50 or more RPPVSM, only 4 patterns qualified the CSR hypothesis. The remaining patterns were clustered. With this result, RPPVSM patterns can be grouped into two: 1) middle to low density patterns with fewer than 50 RPPVSM, and 2) high density patterns with 50 or more RPPVSM. The RPPVSM in the middle to low density patterns tend to follow a CSR distribution, which is independent and uniform, while the RPPVSM in the high density patterns tend to form clusters.

TABLE I. A SUMMARY OF COMPLETE SPATIAL RANDOMNESS (CSR) TEST RESULTS

No. of RPPVSM	**No. of Patterns**	**No. of Patterns Qualified CSR**	**% of Patterns Qualified CSR**	**Demographic Information**
1 to 5	47	N/A	N/A	40 Asians + 4 Caucasians + 2 Latinos + 1 African American
6 to 11	62	55	88.71%	52 Asians + 4 Caucasians + 6 Latinos
12 to 19	40	29	72.5%	31 Asians + 6 Caucasians + 3 Latinos
20 to 29	31	24	77.42%	23 Asians + 5 Caucasians + 3 Latinos
30 to 49	28	16	57.14%	13 Asians + 13 Caucasians + 2 Latinos
50 to 69	19	2	10.53%	8 Asians + 10 Caucasians + 1 Latino
70 to 99	20	1	5.00%	2 Asians + 18 Caucasians
100 or more	22	1	4.55%	22 Caucasians

We also observed that Asians and Latinos tend to have fewer RPPVSM than Caucasians. From 208 patterns which belong to middle to low density group, 84% were from Asians and Latinos, while from 61 patterns which belong to high density group, 82% were from Caucasians. Medical studies point out that race influences the incidence and distribution of nevi [41]-[47]. White subjects (Caucasian) were found to have an average of 14.6 to 61 nevi per subject on their whole body [41]-[43] while Black subjects (African-American) were found to have an average of 2.0 to 11 nevi per subject on their whole body [41]-[45]. Asians (Chinese, Korean, and Japanese) were found to have an average of 2.5 to 16.1 nevi per subject on their whole body [46]-[47]. The numbers of nevi are given in ranges because they are compiled from different studies on over 1000 patients. Due to different sample sizes and various factors affecting the occurrence of nevi (e.g., location, sun exposure, and

age), their statistical results have some fluctuations. These medical studies show that the average number of nevi in Asians is slightly higher than the average number of nevi in Black subjects but significantly lower than the average number of nevi in White subjects. Our statistical results match with the results from these medical studies. Eastern Asians generally have light intermediate skin tone, which would not affect nevi identification. However, their average number of nevi was much lower than the average number of nevi in White subjects. It indicates that the higher number of RPPVSM observed in Caucasian population is not caused by the skin contrast between the lighter-skinned and the darker-skinned subjects. Instead, they are most likely influenced by the racial differences.

C. Independence Test Results and Discussion

The CSR hypothesis test is not reliable for patterns with fewer than 6 RPPVSM, and therefore, the 47 patterns with 1 to 5 RPPVSM in our database were tested for an independent distribution hypothesis only. In this test, we wanted to investigate whether the presence of RPPVSM in a sub-region of the skin is or is not influenced by the presence of other RPPVSM in different sub-regions of the skin. To perform the test, a rather similar approach to the quadrat counts method was implemented. All patterns were divided into 2x2 grids. Then, a contingency table (see Table II) for testing the independence between two grids was built (e.g., grid 1 & grid 2). For testing the independence between grid X and grid Y, if a sample pattern had a RPPVSM in grid X but did not have RPPVSM in grid Y, N_3 was increased by 1. Then, if another sample pattern did not have RPPVSM in both grid X and grid Y, N_1 was increased by 1. The total value of $N_1+N_2+N_3+N_4$ was the total number of samples. For each contingency table, the Pearson chi-square statistic was computed. Using a significance level $\alpha = 0.05$, the hypothesis of independent distribution was accepted if the p-value was greater than 0.05. The results of the independence hypothesis test are summarized in Table III. The computed p-values for all grid pairs are greater than 0.05, meaning that the occurrence of RPPVSM in very low density patterns is an independent event.

We have neither considered the case of weight gain or weight loss nor how it affects the distribution of RPPVSM because our current database cannot support such a study. The CSR test

divides the images into different quadrats and then computes the chi-square statistics. If numbers of RPPVSM in quadrats before and after weight gain (loss) are the same, the chi-square statistics from the two calculations will be the same. In other words, the CSR test will give the same conclusion. Since the CSR test counts number of RPPVSM in each of the quadrats instead of measuring the distance between RPPVSM, it is robust to this distortion. However, if the weight gain (loss) is very significant, an image normalization process should be performed to erase this distortion.

TABLE II. A CONTINGENCY TABLE FOR THE INDEPENDENCE HYPOTHESIS TEST

Grid *Y* / Grid *X*	**RPPVSM = 0**	**RPPVSM > 0**	**Total**
RPPVSM = 0	N_1	N_2	N_1+N_2
RPPVSM > 0	N_3	N_4	N_3+N_4
Total	N_1+N_3	N_2+N_4	$N_1+N_2+N_3+N_4$

TABLE III. A SUMMARY OF *P*-VALUES IN THE INDEPENDENCE HYPOTHESIS TEST

Grid	**1**	**2**	**3**	**4**
1		0.2461	0.0618	0.2012
2			0.6352	0.2012
3				0.7059
4				

IV. A RPPVSM INDIVIDUALITY MODEL

A point matching model to estimate the probability of random correspondence (PRC) of RPPVSM is presented in this section. We focused on middle to low density RPPVSM patterns which qualified the CSR hypothesis because their statistical properties could be accurately modeled. The model was evaluated against empirical results obtained by matching RPPVSM patterns from different subjects. The following assumptions were employed in the model:

1) The locations of RPPVSM followed an independent and uniform distribution.
2) The locations of RPPVSM could not be too close to each other. Two RPPVSM were considered too close if their distance was less than or equal to r_0, where r_0 was a tolerance distance. To realize this assumption, a distance check was performed before matching. Two RPPVSM whose distance was shorter than r_0 were merged as one. The merging was performed by sorting RPPVSM in the *x*-axis direction, then keeping the first RPPVSM for matching while removing the other.
3) There was one and only one correct alignment between an input pattern and a template pattern. Partial matching was not considered since it might result in multiple correct alignments.

4) Each RPPVSM in the input pattern could match one and only one RPPVSM in the template pattern and vice versa. To realize this assumption, if two RPPVSM were matched to the same correspondence RPPVSM, the two RPPVSM were considered as one RPPVSM.
5) A correspondence between two RPPVSM from different persons was an independent event.
6) Each correspondence was equally important. Correspondences in the peripheral area were weighted equal to those in the center area.
7) Only positive correspondences were considered. Conflicting evidence (i.e., a RPPVSM in the input pattern does not correspond to any RPPVSM in the template pattern) was not considered.
8) The quality of all images was equally good for manual RPPVSM detection. A salient feature labeled as a RPPVSM in the first image had a correspondence in the second image and vice versa.

Our objective is to compute the probability that, given an input pattern with n RPPVSM, any arbitrary (template) pattern with m RPPVSM from a different person will have exactly p correspondences with the input pattern. The correspondences are established as follows. Taking only RPPVSM locations as the feature for matching, an input pattern I and a template pattern T can be defined as

$$I = \left\{ \left(x_{i1}, y_{i1} \right), \left(x_{i2}, y_{i2} \right), ... \left(x_{in}, y_{in} \right) \right\}, \tag{2}$$

$$T = \left\{ \left(x_{t1}, y_{t1} \right), \left(x_{t2}, y_{t2} \right), ... \left(x_{tm}, y_{tm} \right) \right\}. \tag{3}$$

Assuming that I and T have been aligned, correspondence point pairs should be located near each other. A correspondence between the a^{th} RPPVSM in the input pattern and the b^{th} RPPVSM in the template pattern is established if and only if

$$\sqrt{(x_{tb} - x_{ia})^2 + (y_{tb} - y_{ia})^2} \le r_0, \tag{4}$$

where r_0 is a tolerance distance. Even when two aligned patterns are from the same subject, the correspondence points may slightly deviate from one another due to local variations in the patterns. The parameter r_0 is introduced to accommodate these intra-class variations. Two points will still be allowed to match if a correspondence point is located within the tolerance distance of the other point. Fig. 3 illustrates a genuine match, where all correspondence pairs can be identified. Each

correspondence pair is connected by a line, and each input RPPVSM is within the tolerance region $C = \pi r_0^2$ of its correspondence template RPPVSM. The dashed line area indicates the overlap area A between the input and the template patterns after alignment.

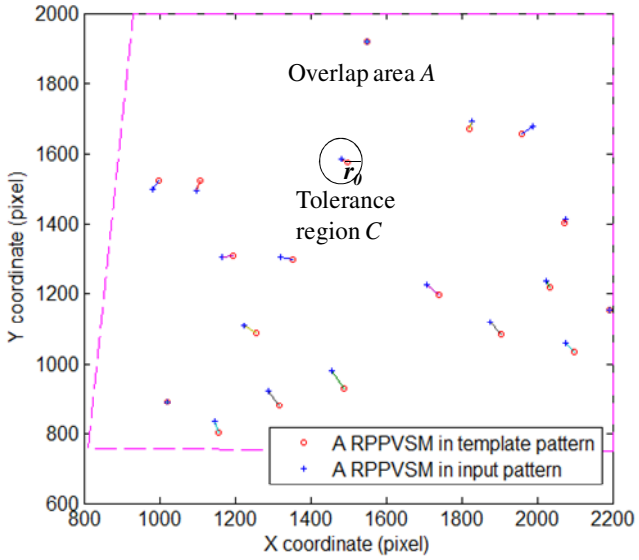

Fig. 3. An illustration of the overlap area A and the tolerance region C in aligned input and template RPPVSM patterns. The established correspondences are connected by lines.

Now we present our model for estimating the probability of random correspondence. Let $d = \sqrt{(x_t - x_i)^2 + (y_t - y_i)^2}$ be the Euclidean distance between any two arbitrary points (x_i, y_i) and (x_t, y_t) in the input and template patterns, respectively. The locations of the input and template RPPVSM are independent, because they are from different subjects. Thus, the probability that (x_i, y_i) falls within the tolerance region of (x_t, y_t), i.e., $d \le r_0$ is

$$Pr(d \le r_0) = \pi r_0^2 / A = C / A . \tag{5}$$

If an input pattern has two RPPVSM and a template pattern has m RPPVSM, the probability that the first input RPPVSM has a correspondence with one of the m template RPPVSM is mC/A, and the probability that the second input RPPVSM does not have a correspondence is $(A - mC)/(A - C)$. Thus, the probability that there is exactly one correspondence (and one non-correspondence) between the two patterns is given by

$$Pr(A, C, m, 2, 1) = 2 \times (mC/A) \times ((A - mC)/(A - C)). \tag{6}$$

The probability is multiplied by 2 since two scenarios are possible — the first input RPPVSM has a correspondence but the second input RPPVSM does not have a correspondence, or vice versa.

Extending the scenario to an input pattern with n RPPVSM, the probability that exactly one input RPPVSM has a correspondence with one of the m template RPPVSM can be calculated as the probability of having one correspondence multiplied by the probability of having no other correspondences. Thus, if the input pattern has n RPPVSM and the template pattern has m RPPVSM, the probability of obtaining exactly one correspondence is

$$Pr(A,C,m,n,1)=\binom{n}{1}\times\left(\frac{mC}{A}\right)\times\left(\frac{A-mC}{A-C}\right)\left(\frac{A-(m+1)C}{A-2C}\right)\ldots\left(\frac{A-(m+((n-1)-1))C}{A-(n-1)C}\right). \tag{7}$$

Now we generalize the model for the scenario with more than one correspondence. Given an input pattern with n RPPVSM and a template pattern with m RPPVSM, the probability that there are exactly p correspondences, where $p\in\{0,1,\ldots\min(m,n)\}$, and the probability that the remaining n-p points do not have correspondences is

$$\begin{aligned}Pr(A,C,m,n,p)=&\binom{n}{p}\times\left(\frac{mC}{A}\right)\left(\frac{(m-1)C}{A-C}\right)\left(\frac{(m-2)C}{A-2C}\right)\ldots\left(\frac{(m-(p-1))C}{A-(p-1)C}\right)\\ &\times\left(\frac{A-mC}{A-pC}\right)\left(\frac{A-(m+1)C}{A-(p+1)C}\right)\left(\frac{A-(m+2)C}{A-(p+2)C}\right)\ldots\left(\frac{A-(m+((n-p)-1))C}{A-(n-1)C}\right).\end{aligned} \tag{8}$$

Let M = [A/C], where [] represents an operator of rounding to the nearest integer. Since A>>C, $M\approx A/C$. Dividing all numerators and denominators by C, Eq. 8 can be written as

$$\begin{aligned}Pr(M,m,n,p)=&\binom{n}{p}\times\left(\frac{m}{M}\right)\left(\frac{m-1}{M-1}\right)\left(\frac{m-2}{M-2}\right)\ldots\left(\frac{m-(p-1)}{M-(p-1)}\right)\\ &\times\left(\frac{M-m}{M-p}\right)\left(\frac{M-m-1}{M-(p+1)}\right)\left(\frac{M-m-2}{M-(p+2)}\right)\ldots\left(\frac{(M-m)-((n-p)-1))}{M-(n-1)}\right),\end{aligned} \tag{9}$$

which finally reduces to the following hypergeometric distribution

$$Pr(M,m,n,p)=\frac{\binom{m}{p}\binom{M-m}{n-p}}{\binom{M}{n}}. \tag{10}$$

The above model was previously used to estimate the probability of random correspondence in fingerprints [28]. However, when compared to the empirical results, the theoretical probabilities were much smaller than the empirical probabilities. It was explained in [28]-[29] that the assumption of independent and uniform distribution of minutiae did not reflect the actual tendency of minutiae which in fact form clusters, thus resulting in overestimation of fingerprint individuality. Based on the statistical results reported in section III, this individuality model is more suitable for RPPVSM since the assumption fits the empirical distribution of middle to low density RPPVSM patterns.

V. A RPPVSM MATCHING METHOD

A RPPVSM matching method involves registering an input pattern to a template pattern and establishing correspondences based on a tolerance distance r_0. There are two types of transformations for image registration [48]. One is the global mapping model and the other is the local mapping model. The former applies the same transformation to the whole image while the latter allows local variations. Since the images used in this study were taken in a standard pose, local variations were very small and thus could be ignored. Major variations came from the camera's position, zoom factor, and view angle, which can be handled by rotation, scale, and translation operations. Therefore, an affine transformation, which is a global mapping model, was selected to handle the registration process. The affine transformation is defined as

$$\begin{bmatrix} u \\ v \end{bmatrix} = \begin{bmatrix} a_1 & a_2 & a_3 \\ b_1 & b_2 & b_3 \end{bmatrix} \begin{bmatrix} x \\ y \\ 1 \end{bmatrix}, \tag{11}$$

where (u, v) is the transformed coordinate of (x, y) and $\begin{bmatrix} a_1 & a_2 & a_3 \\ b_1 & b_2 & b_3 \end{bmatrix}$ is a parameter matrix that can be obtained by solving the above linear equation. The parameter matrix was determined by performing a registration of non-RPPVSM points from the input and the template patterns, which are called registration points. These registration points were obtained in the following way:

1) For each point set I and T, a Voronoi diagram was generated. Since Voronoi diagrams can be considered as internal graph structures which are different for each pattern, we made the alignment insensitive to rotation variation by using this diagram to generate registration points.

Registration points were the vertices of the Voronoi diagram (marked as '+' in Fig. 4b) located within a bounding box formed by the top, bottom, most left, and most right RPPVSM. The bounding box is the rectangular area denoted by the dashed line.

2) To obtain a stable alignment, more points were added as registration points. The points were generated from the middle of the lines connecting the most left RPPVSM with the rest RPPVSM (see Fig. 4(c)). Similarly, the middle points of the lines connecting the most right, top, and bottom RPPVSM with the rest RPPVSM were also added (see Figs. 4(d)-(f)). This scheme works under the assumption that the four RPPVSM forming the bounding box can be recognized in different images of the same person. Full back torsos could be seen in our images and the RPPVSM were recognized by our medical researchers. Thus, this assumption could be fulfilled.

The registration points from the input pattern were aligned to the registration points from the template pattern using the Coherent Point Drift (CPD) algorithm with affine transformation [49] (see Figs. 5(a)-(c)). Using the obtained affine transformation parameters, the RPPVSM in the input pattern I were subsequently aligned to the template pattern T (see Figs. 5(d)-(f)). Candidate correspondences between the template and the input RPPVSM were searched using a k-Nearest Neighbor algorithm with $k = 1$ and a correspondence was accepted if $d \leq r_0$. The matching result is illustrated in Fig. 5f. The correspondences are connected by lines and the overlap area is denoted by the dashed lines. Only RPPVSM located inside the overlap area were considered in the matching.

A. *Estimation of* r_0

Five parameters A, C, m, n, and p are required by the model. The values of A, m, and n are obtained from the matching experiment. A is the intersection area between the input and the template patterns after alignment, and m and n are respectively the number of RPPVSM in the template pattern and the input pattern within the overlap area. The value of p ranges from 0 to min(m, n). The value of C depends on the tolerance distance r_0. To determine r_0, we matched the genuine RPPVSM patterns in our database and obtained the distribution of their correspondence distances as given in Fig. 6. It should be noted that there is no natural impostor correspondence. The impostor correspondence depends on r_0 and the matching algorithm. Images collected in the first session were used as the

templates and the images collected in the second session were used as the inputs. Let (x_i, y_i) be a RPPVSM in an input pattern and (x_t, y_t) be a RPPVSM in a template pattern. r_0 is determined from $Pr\left(\sqrt{(x_t - x_i)^2 + (y_t - y_i)^2} \le r_0\right) \ge t$, where t is a statistical threshold. From 94 genuine pairs of middle to low density RPPVSM patterns which qualified the CSR test, we obtained r_0 = 86.82 pixels and r_0 = 69.70 pixels for t = 97.5% and t = 95%, respectively.

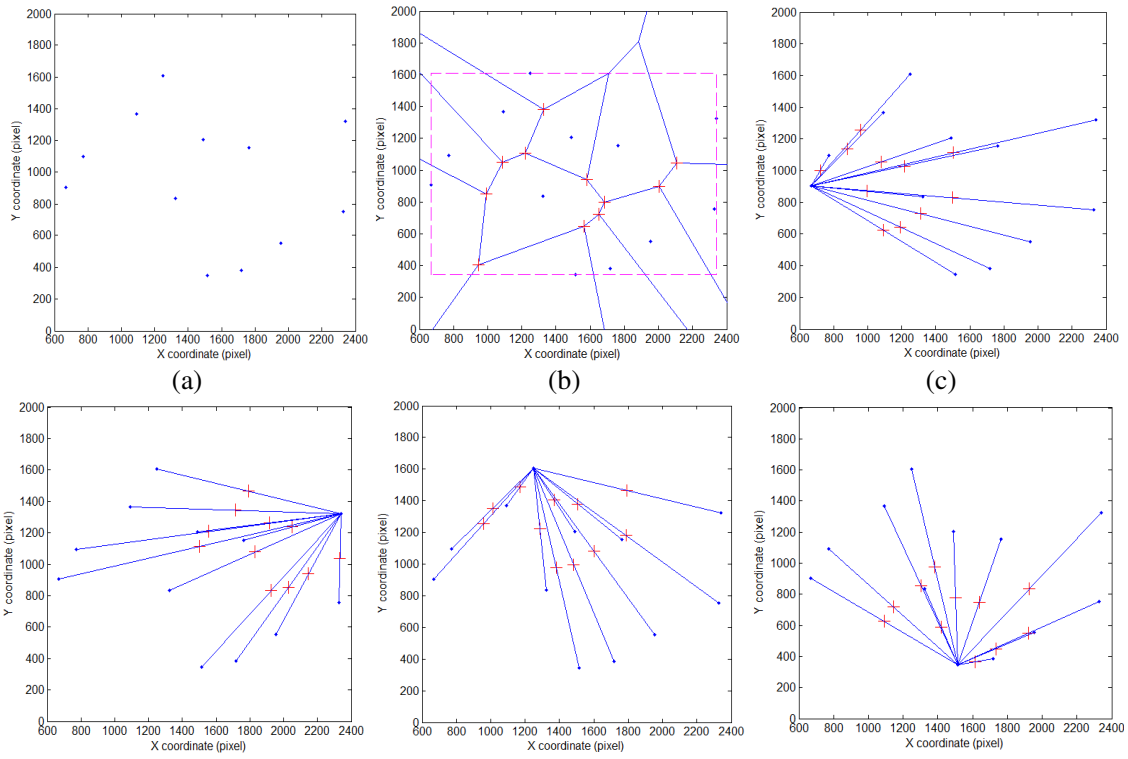

Fig. 4. Steps to generate registration points from a pattern (registration points are labeled '+'); (a) the original RPPVSM, (b) a Voronoi diagram of the RPPVSM in (a) — registration points are the Voronoi vertices within the dashed line boundary, (c)-(f) respectively lines connecting the most left, the most right, the top, and the bottom RPPVSM with the rest RPPVSM. The additional registration points are the middle of these lines.

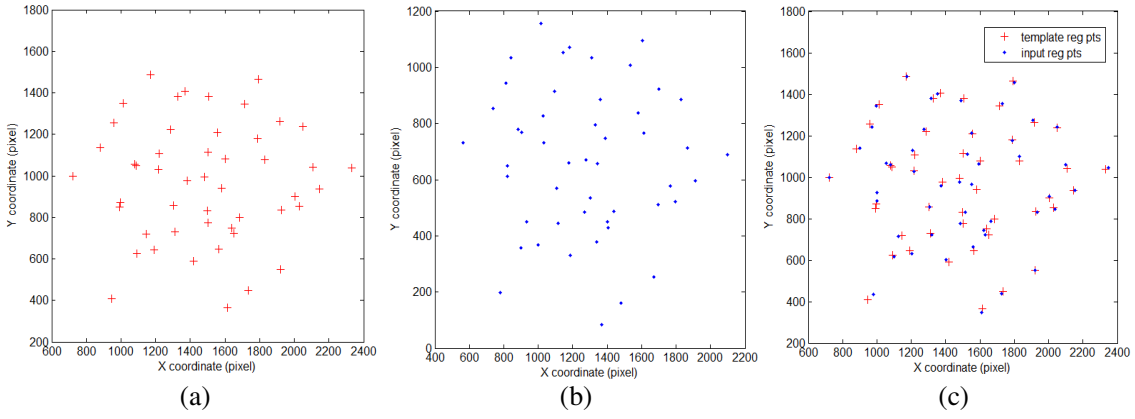

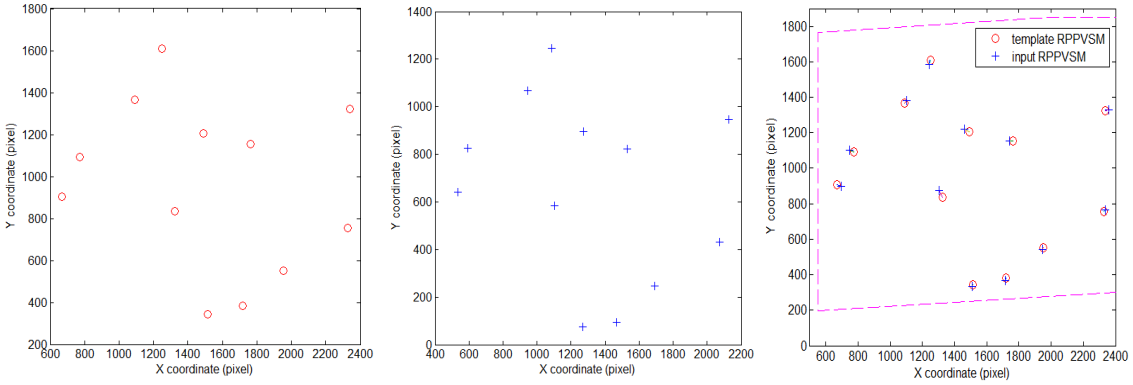

(d) (e) (f)

Fig. 5. Illustration of the matching method: (a) registration points from a template pattern, (b) registration points from an input pattern, (c) the result of alignment, (d) RPPVSM in the template pattern, (e) RPPVSM in the input pattern, and (f) the matched RPPVSM indicated by the connected lines within the overlap area, which is denoted by the dashed lines.

VI. EXPERIMENTAL RESULTS

Empirical random correspondences were obtained by matching impostor pairs of middle to low density RPPVSM patterns which qualified the CSR hypothesis. We grouped 269 patterns in the database into middle to low density patterns (208 subjects with < 50 RPPVSM) and high density patterns (61 subjects with ≥ 50 RPPVSM). From the 208 subjects in the middle to low density RPPVSM group, we selected 124 subjects whose patterns qualified the CSR hypothesis for the individuality study. Since 30 subjects only had one image (from LA database), the total number of images used in this study became 218 images (124 images from session 1 + 94 images from session 2). 11,562 impostor matches were generated from 124 template images and 94 input images. In this section, we first report our matching results and then evaluate the RPPVSM individuality model by comparing the empirical results to the model estimations.

A. *Matching Performance*

For the matching experiment, r_0 was set to 80 pixels, which was obtained by rounding down the correspondence distance at t = 97.5% to the nearest ten. The value was rounded down to reduce the number of points that would be merged. The matching score was calculated using $2p/(m+n)$, where p is the number of correspondences, m is the number of RPPVSM in a template pattern, and n is the number of RPPVSM in an input pattern. Fig. 7 shows the receiver operating characteristic (ROC)

curve of the genuine and the impostor matchings. When the genuine acceptance is 96.81%, which is at matching score of 0.77, the corresponding false acceptance rate is 0.17%. Some genuine pairs could not be matched, because r_0 was selected to cover less than 97.5% of the genuine correspondences. Moreover, some impostor matches had high scores due to small numbers of RPPVSM in the patterns.

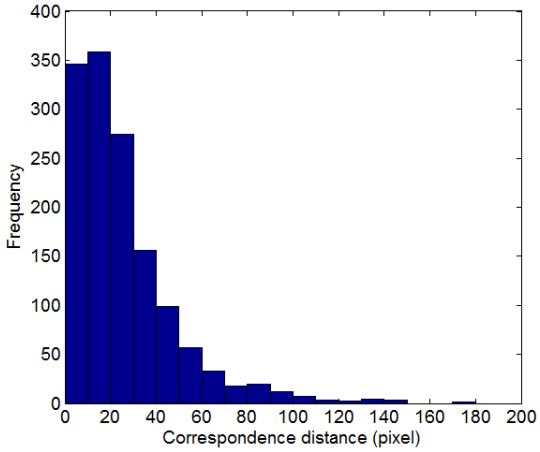

Fig. 6. The distribution of correspondence distances from 94 genuine pairs of RPPVSM patterns to determine r_0.

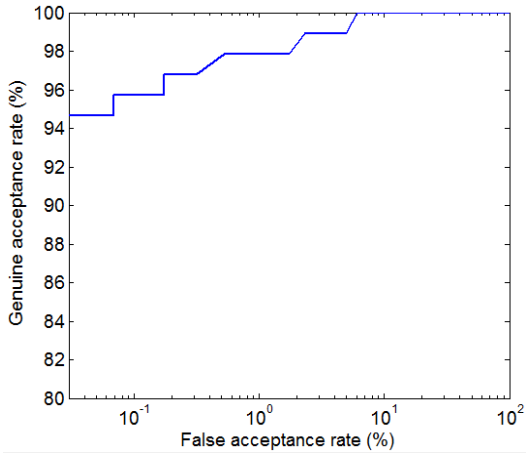

Fig. 7. The ROC curve of RPPVSM matching.

B. Model Evaluation

A set of parameters $M_i, m_i,$ and n_i and an empirical random correspondence $p_i \in [0, \min(n_i, m_i)]$ were generated from each impostor matching. With the parameter sets from different impostor matchings, the distribution of random correspondence can be estimated. Let X_i be a random variable and $Pr(X_i = p \mid M_i, m_i, n_i) = Pr(M_i, m_i, n_i, p)$. If the theoretical model is correct, the empirical distribution can be approximated by

$$Pr(p) = \frac{1}{N} \sum_{i=1}^{N} Pr(M_i, m_i, n_i, p), \tag{12}$$

where N is the number of impostor matchings. To standardize the unit for comparison, the theoretical probabilities were multiplied by N to obtain the frequencies of random correspondences. Eq. 12 is the average of the individual distributions with different parameter sets. Then, the difference between the theoretical and the empirical distributions was evaluated based on the 95% confidence interval of the theoretical frequency distribution. The confidence interval was generated as follows:

1) Let R_i be an observation of a random sample from the distribution $Pr(X_i|M_i,m_i,n_i)$, where $i = 1,\ldots, N$. By counting the number of R_i with p random correspondences, where $p \in [0, \max_i(\min(n_i, m_i))]$, a frequency distribution was obtained.
2) Step 1 was repeated 3000 times to obtain a stable sampling result. Thus, we had 3000 frequency distributions.
3) Let $F_j(p)$ be the frequency of p random correspondences from the j^{th} sampling process. Given a fixed p, each $F_j(p)$ could be considered as an observation from a one-dimensional distribution and its 2.5 percentile and 97.5 percentile were used to form the 95% confidence interval.

Even though in this experiment all the original RPPVSM patterns qualified the CSR test, if the overlap area A was small (i.e., less than 10% of the average value of A) or the RPPVSM inside the overlap area were too few (i.e., $m < 4$ or $n < 4$), the RPPVSM patterns inside the overlap area might no longer qualify the CSR hypothesis. Thus, matchings with small values of A, n, or m were excluded. After the exclusion, 9,697 sets of parameters were kept for model evaluation.

Fig. 8a shows the empirical and theoretical frequency distributions of the RPPVSM random correspondences using $r_0 = 80$ pixels, which is about 4% of the average torso heights in our database. It can be seen that the theoretical distribution fits the empirical distribution very well. More precisely, the empirical results are within the 95% confidence interval of the theoretical results. This implies that their difference is statistically insignificant. To confirm the result, we repeated the experiments using $r_0 = 75$ pixels (see Fig. 8b), whose corresponding statistical threshold was smaller but still in the range of $t = 95\%$ and $t = 97.5\%$ to maintain a similar matching performance with $r_0 = 80$ pixels. The plot shows consistency with the previous result, where all empirical results are within the 95% confidence interval of the theoretical results.

VII. Predicted Error Rates for Verification and Identification

Verification (one-to-one matching) and identification (one-to-many matching) are two important scenarios in forensic investigation. Verification is performed when a suspect is in custody or is available for comparison, while identification is performed when law enforcement officers search for a suspect in a previously existing database. Since the probability of random correspondence measures

the likelihood of finding a similar RPPVSM pattern from two different persons, the verification error rate can be estimated by Eq. 10 directly.

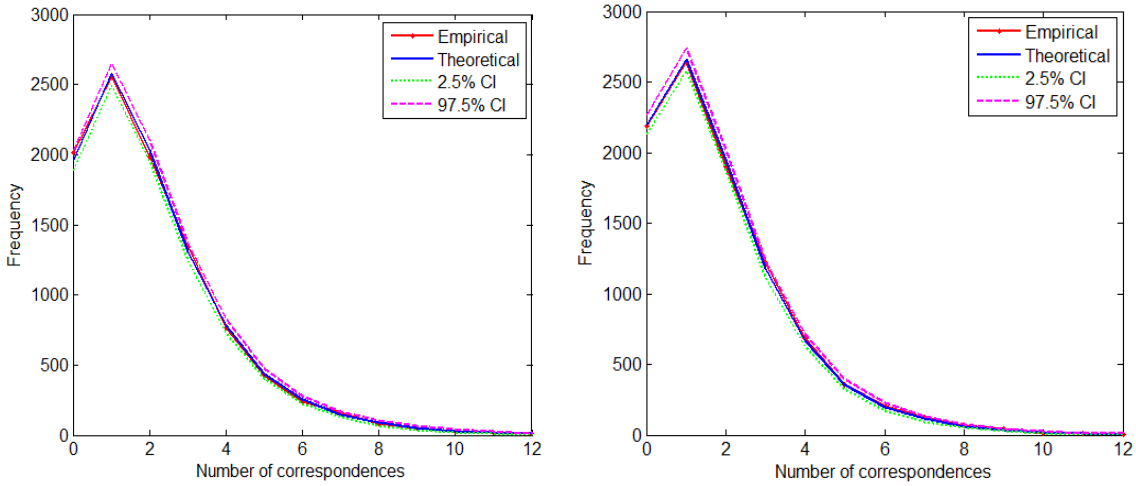

Fig. 8. Comparison of the empirical and theoretical random correspondences for (a) r_0 = 80 pixels (4% of average torso height) and (b) r_0 = 75 pixels (3.75% of average torso height).

A. Verification

In the database used for this study, the average number of RPPVSM in the middle to low density patterns is 22. We started the error rate estimation with this average value (i.e., m=22, n=22, p=22). Subsequently, the number of RPPVSM was gradually decreased to predict the lower bound for reliable verification. The value of A was set to 1.5×10^6 pixels^2, which was the mean value of A in the impostor matching experiment. The value of r_0 was set to 80 pixels, based on the value used in the experiment above. Since evidence images (input) are typically of poorer quality than reference images (template), which can be collected from suspects directly in a controlled setting, we considered the cases when $n < m$.

The probabilities of random correspondence with different RPPVSM configurations are given in Table IV. Non-matched events increase the probability of random correspondence significantly. For example, in Table IV(a), when one RPPVSM is not matched (m=22, n=22, p=21), the probability of random correspondence increases by 3 orders of magnitude from the full match (m=22, n=22, p=22). Then, when only 18 out of 22 RPPVSM are matched, the probability increases by 9 orders of magnitude. The same trend can be seen from the other tables. The probability of random correspondence also increases when a few RPPVSM are missing due to poor image quality. For

example, when only 18 out of 22 RPPVSM can be identified from the input image and all of them can be matched (m=22, n=18, p=18), the probability of random correspondence increases by 5 orders of magnitude compared to the ideal full match scenario (m=22, n=22, p=22). It can be seen that for all full match scenarios highlighted in Table IV (e.g., from m=22, n=22, p=22 to m=7, n=7, p=7), the probabilities of random correspondence are not greater than 5.04×10^{-10}.

B. Identification

The probability of false identification also called the *False Positive Identification Rate* (*FPIR*), can be estimated by $1-\prod_{i=1}^{h}(1-Pr(M_i,m_i,n_i,p))$, where h is the size of database and each set of (M_i, m_i, n_i) is generated from matching an input RPPVSM pattern with one template RPPVSM pattern in the database. In the following calculations, we assumed that all (M_i, m_i, n_i) were the same and therefore, the probability of false identification could be estimated by $1-(1-Pr(M,m,n,p))^h$. We set the value of M based on the average value of A in the impostor matching experiment and r_0 = 80 pixels. We considered full match scenarios where $m_i = n_i = p$ (e.g., m=7, n=7, p=7).

Table V lists probabilities of false identification with different RPPVSM configurations and different database sizes. A full match with 7 RPPVSM in a database containing 100 persons gives a performance with error rate of 5.04×10^{-8}. However, when 7 RPPVSM are used to identify a person in a database with 100 million people, the error rate is 0.049. With this database size, a full match with 16 RPPVSM gives an error rate of 1.11×10^{-8}.

TABLE IV. THEORETICAL PROBABILITIES OF RANDOM CORRESPONDENCE WITH DIFFERENT RPPVSM CONFIGURATIONS

(A) ***m*=22**

n \ ***p***	**18**	**19**	**20**	**21**	**22**
22	4.15e-10	6.99e-12	6.16e-14	2.26e-16	1.94e-19
21	8.15e-11	1.01e-12	5.82e-15	1.05e-17	N/A
20	1.25e-11	1.02e-13	2.88e-16	N/A	N/A
19	1.35e-12	5.37e-15	N/A	N/A	N/A
18	7.65e-14	N/A	N/A	N/A	N/A

(B) ***m*=17**

n \ *p*	**13**	**14**	**15**	**16**	**17**
17	3.40e-08	7.07e-10	7.58e-12	3.32e-14	3.37e-17
16	8.59e-09	1.31e-10	9.23e-13	1.99e-15	N/A
15	1.72e-09	1.73e-11	5.96e-14	N/A	N/A
14	2.46e-10	1.21e-12	N/A	N/A	N/A
13	1.88e-11	N/A	N/A	N/A	N/A

(C) ***m*=12**

n \ *p*	**8**	**9**	**10**	**11**	**12**
12	1.13e-05	3.34e-07	4.93e-09	2.89e-11	3.83e-14
11	4.01e-06	8.77e-08	8.49e-10	2.45e-12	N/A
10	1.17e-06	1.67e-08	7.96e-11	N/A	N/A
9	2.48e-07	1.75e-09	N/A	N/A	N/A
8	2.93e-08	N/A	N/A	N/A	N/A

(D) ***m*=7**

n \ *p*	**3**	**4**	**5**	**6**	**7**
7	0.0144	8.84e-04	2.41e-05	2.40e-07	5.04e-10
6	0.0087	3.96e-04	7.09e-06	3.48e-08	N/A
5	0.0046	1.38e-04	1.22e-06	N/A	N/A
4	0.0020	2.88e-05	N/A	N/A	N/A
3	5.18e-04	N/A	N/A	N/A	N/A

TABLE V. THEORETICAL PROBABILITIES OF FALSE IDENTIFICATION WITH DIFFERENT RPPVSM CONFIGURATIONS AND DATABASE SIZES

Size of database, *h*	***m*=7, *n*=7, *p*=7**	***m*=10, *n*=10, *p*=10**	***m*=12, *n*=12, *p*=12**	***m*=14, *n*=14, *p*=14**	***m*=16, *n*=16, *p*=16**
100	5.04e-08	1.21e-10	3.83e-12	1.78e-13	1.11e-14
1,000	5.04e-07	1.21e-09	3.83e-11	1.78e-12	1.11e-13
10,000	5.04e-06	1.21e-08	3.83e-10	1.78e-11	1.11e-12
100,000	5.04e-05	1.21e-07	3.83e-09	1.78e-10	1.11e-11
1 million	5.04e-04	1.21e-06	3.83e-08	1.78e-09	1.11e-10
10 million	0.0050	1.21e-05	3.83e-07	1.78e-08	1.11e-09
100 million	0.0492	1.21e-04	3.83e-06	1.78e-07	1.11e-08

VIII. DISCUSSION

This paper presents an individuality model for the independently and uniformly distributed RPPVSM patterns. Our model estimates that the probability of two persons both having 7 RPPVSM all being matched is very low. From the 269 subjects involved in our study, 213 had at least 7 RPPVSM on their backs. This is almost 80% of subjects in our database. It indicates that in general circumstances, when there is enough skin for observation, identification using RPPVSM is possible.

The model can tolerate and account for some intra-class variability. When some RPPVSM in two images from the same subject are missing or not matched (see Table IV), the probabilities of random correspondence were also estimated. In this scenario, the probability of random correspondence will increase. However, depending on the threshold and the number of non-matched RPPVSM, the probability can still be sufficiently low for positive verification. In actual practice, depending on certain variables (e.g., r_0) and other circumstances, low numbers of RPPVSM may be sufficient for verification. RPPVSM can be combined with other biometric traits (e.g., tattoos [6]-[8] or vein patterns [9]) if they are available, especially in the cases when there are only a limited number of RPPVSM.

Our work makes a significant improvement over a prior study using manual annotation for facial marks where high inter-observer error was reported [15]. The list of skin marks in [15] included many types of non-medical and non-scientific skin features, where many had ambiguous definitions. For example, raised skin was defined as "a solid raised mark less than 1 cm across. It has a rough texture and appears in red, pink, or brown in color". They also included pimples, which are in fact a transient skin disease. The medical significance and the biological behavior of the specific skin marks chosen for biometrics are critical to consider. In this study, we considered only four types of carefully chosen skin marks, which are nevi (moles), lentigines, cherry hemangiomas, and seborrheic keratoses. These skin features are medically well-defined and relatively easy for dermatologists to identify by clinical observation alone. In addition to the features of the skin marks, the ability of trained medical professionals to accurately, confidently, and reproducibly identify them from images will affect the confidence level of the results. Srinivas et al. [15] provided the definitions of their skin features with a few sample images to their untrained observers. Our annotation process was carried out by medical researchers led by an American Board of Dermatology-certified dermatologist. In fingerprint identification, fingerprint experts may have different opinions on the presence of minutiae, especially when dealing with low quality images [50]. However, the variability that might occur between different fingerprint experts is minimized through years of training. Although specific training programs for identifying RPPVSM were not employed for this work, the ability to accurately identify the individual components of RPPVSM (nevi, angiomas, etc.) is included in the board certification

process in the United States. Additionally, the ability to accurately diagnose pigmented and vascular skin marks from digital images has been studied extensively as part of the validation of telemedicine practices [51]. Because of these significant differences in content and procedure, the results reported in [15] may not be applicable to our work.

One may argue that this study focused on CSR patterns with middle to low density only and therefore the model may not be applicable to other RPPVSM patterns. We do not propose a universal model because RPPVSM patterns have different statistical properties. In fact, the beauty of our study lies on the fact that we used only RPPVSM patterns which matched the model assumptions. The estimation capability of our model is far stronger than many previous fingerprint individuality models. In those studies, fingerprint individuality was estimated based on a set of statistical assumptions which did not match statistical properties of fingerprint. In our study, a statistical test was performed to guarantee that the selected data and the model assumptions match well. As a result, the model estimations fit the empirical results very well (Fig. 8). The individuality of RPPVSM should be further studied and new models should be developed for the RPPVSM patterns which were excluded. Note that the individuality of other biometric traits (e.g., fingerprint, face, and iris) is still being studied.

Although full back torsos were employed in this study, the method can be applied to partial back or other body parts (e.g., arms or thighs). The statistical model presented in this paper neither specifically focuses on the body location nor assumes any prior knowledge of the skin of the torso. In the legal case mentioned in section I, RPPVSM were identified from the left thigh of the criminal in evidence images. Verification was performed using photos of the entire body of the arrested suspect in poses simulating the position of the criminal in evidence images. In the future, if there are subject pose or camera viewpoint variations in evidence images, a 3D model may be used to transform the images into a standard pose and viewpoint so that the result in this paper can be applied directly.

Regarding the database, one may raise a concern that our study covered three different races (i.e., Caucasian, Asian, and Latino) but did not include Black subjects, which according to the U.S. Bureau of Justice Statistics, represent about 40% of prison inmates [52]. The authors acknowledge that not including Black subjects is one limitation of this study. However, in child sexual exploitation cases,

which are the emphasis in this paper, 76% of defendants are White and only 5% of defendants are Black [3]. Moreover, this study is not specific to the United States because child sexual offenses could happen in any countries (e.g., Japan [53], England [54], and Australia [55]).

In this paper, RPPVSM is used for forensic applications. We would like to highlight their difference from commercial/governmental applications. Jain et al. [56] mentioned five factors of a biometric trait; two of them are universality and measurability. These factors are important for commercial/governmental applications (e.g., border control and access control). However, in forensic investigations, some biometric traits may be available in evidence and have information for identification, but they may not be considered universal. For example, tattoos have been regularly used in legal cases but not everyone has tattoos. When tattoos are available in evidence images, law enforcement agents use them for identification. Similarly, when evidence images have RPPVSM, they can be used for identification. 98.90% of the subjects in our study have at least one RPPVSM. Moreover, nevi have been medically studied in various races [41]-[47]. These two facts indicate the universality of RPPVSM. In terms of measurability, RPPVSM is a subset of skin marks and skin marks have been used in legal cases. Besides the previously mentioned legal case [17], we have also identified skin marks in evidence images of other cases provided by our law enforcement partners. In a news release by the U.S. Immigration and Customs Enforcement (ICE), an image showing a mole (nevus) on the left inner thigh of a criminal in a child pornography case was released to the public for identification [57]. The mole can be seen clearly in the image. They show that RPPVSM are measurable in evidence images.

For this study, original images were captured by digital cameras with different resolutions but were normalized to the smallest resolution of 6 Megapixels, which is still compatible with the resolution of high-definition video cameras (2 Megapixels). Furthermore, since the key for identifying RPPVSM is on resolution in terms of dpi (dot per inch), not number of pixels, and many evidence of child sexual offenses show close-up images, lower resolution images are still enough for RPPVSM identification.

This paper aims to study some of the concerns raised in the previously mentioned legal case. However, publishing this paper does not imply that RPPVSM or the proposed model can always be

used in legal cases with skin images. In general legal proceedings, new scientific theories/methods have to be examined in Daubert hearings before they can be used in trials. A Daubert hearing is a session within a trial conducted before a judge only to evaluate the reliability of new scientific theories/methods recommended by prosecutors or defendants in a legal case. Expert witnesses are recruited by prosecutors and defendants to discuss the suitability of the new theories/methods for the particular legal case based on the evidence. The final acceptance or rejection of the theories/methods is decided by the judge based on the expert witnesses' discussion and the evidence. Currently, there is still no scientific study about the individuality of RPPVSM. In fact, there is even no scientific study about the individuality of skin marks. Thus, this paper contributes to initiate legal discussions on this matter.

For operational scenarios, some topics including but not limited to image/video quality, expert knowledge, and training schemes need to be studied in the future. To solve image compression problems, algorithms to remove JPEG artifacts in skin images are available [58]. However, for low resolution, motion blur, and video compression problems, further research is required. Note that in this study, we assumed that "evidence" images were not modified. If criminals put make-up on skin marks or modify evidence images/videos, skin marks can be hidden or even faces can be swapped. In these cases, image forensic techniques can be applied to authenticate tampering in evidence images.

Our future work includes the development of an automated RPPVSM detection technique. Manual identification by experts can be time-consuming. Thus, an automated method will be helpful to speed up the identification process. The technique will include preprocessing, skin marks detection, and RPPVSM classification. In the preprocessing stage, images are normalized for illumination, pose, scale, and resolution. Then, RPPVSM candidates are located by applying blob detection techniques. These candidates are subsequently classified into RPPVSM and non-RPPVSM based on a set of features (e.g., color, contrast, etc.). The classification schemes may range from rule-based to training-based classification. In the matching, more features besides location (e.g., RPPVSM type, color, and size) can be further exploited to increase the discriminative power of RPPVSM. However, the use of these additional features may require higher image quality and will require additional studying and modeling. As with fingerprint identification, the automated method can be used to retrieve a small set

of suspects from a database and the final authentication can be handled by experts because they are expected to provide higher accuracy.

IX. CONCLUSION

This work describes the use of RPPVSM as a novel biometric trait. RPPVSM are common but their uniqueness had not been studied before. We propose in this study an individuality model for the independently and uniformly distributed (CSR) patterns. The results demonstrated that the model accurately fits the empirical random correspondences, signifying that it predicts the empirical results accurately. Therefore, given images with similar properties as our database images, if the identified RPPVSM form middle to low density patterns and pass the CSR test, the proposed model can accurately predict their random correspondences. For CSR patterns with other properties (e.g., images have different resolutions or compression ratios, or a subject's race is different from the races in the database), the model should be re-examined using data with similar properties. With this model, the potential error rates of using RPPVSM patterns for verification and identification were also estimated. Our result showed that the error rates can be very small. These results are important as they show the potential of RPPVSM for forensic investigations. As this paper is preliminary work on RPPVSM, further research is required. Future work will include extension of the database population, image/video quality assessment, and development of an automated method for RPPVSM identification.

ACKNOWLEDGMENT

We would like to thank the U.S. Department of Justice, the U.S. Immigration and Customs Enforcement, the Singapore Prison Service, and the Singapore Police Force for providing legal and forensics information. This work is partially supported by Academic Research Fund Tier 1 (RG6/10) from the Ministry of Education, Singapore.

REFERENCES

[1] The Guardian, "London Riots: The Third Night – Monday 8 August 2011," 8 Aug 2011. Available: http://www.guardian.co.uk/uk/blog/2011/aug/08/london-riots-third-night-live

[2] The Guardian, "Occupy Protest in Rome Hijacked by Rioters who Cause Damage Put at €2m," 16 Oct 2011. Available: http://www.guardian.co.uk/world/2011/oct/16/rome-riot-damage-ringleaders-police

[3] M. Motivans and T. Kyckelhahn, "Federal Prosecution of Child Sex Exploitation Offenders, 2006," *Bureau of Justice Statistics Bulletin*, pp. 1-8, 2007.

[4] BBC News, "International Child Porn Ring Smashed," 26 March 2001. Available: http://news.bbc.co.uk/1/hi/world/americas/1244457.stm
[5] Canada's National Tipline for Reporting the Online Sexual Exploitation of Children Statistics. Available: http://www.cybertip.ca/pdfs/fact_sheet_pdfs/English/CyberStats_en.pdf
[6] A.K. Jain, S.C. Dass, and K. Nandakumar, "Soft Biometric Traits for Personal Recognition Systems," in *Proc. Int. Conf. Biometric Authentication*, pp. 731-738, Hong Kong, 2004.
[7] J.E. Lee, A.K. Jain, and R. Jin, "Scars, Marks and Tattoos (SMT): Soft Biometric for Suspect and Victim Identification," in *Proc. Biometrics Symposium*, pp. 1-8, Tampa, Florida, 2008.
[8] J.E. Lee, R. Jin, A.K. Jain, and W. Tong, "Image Retrieval in Forensics: Tattoo Image Database Application," *IEEE Multimedia*, vol. 19, no. 1, pp. 40-49, 2012.
[9] C. Tang, A.W.K. Kong, and N. Craft, "Uncovering Vein Patterns from Color Skin Images for Forensic Analysis," in *Proc. IEEE CVPR*, pp. 665-672, Colorado Springs, 2011.
[10] D. Lin and X. Tang, "Recognize High Resolution Faces: From Macrocosm to Microcosm," in *Proc. IEEE CVPR*, pp. 1355-1362, New York, 2006.
[11] J.S. Pierrard and T. Vetter, "Skin Detail Analysis for Face Recognition," in *Proc. IEEE CVPR*, pp. 1-8, Minneapolis, 2007.
[12] A.K. Jain and U. Park, "Facial Marks: Soft Biometric for Face Recognition," in *Proc. IEEE ICIP*, pp. 37-40, Cairo, Egypt, 2009.
[13] Z. Zhang, S. Tulyakov, and V. Govindaraju, "Combining Facial Skin Mark and Eigenfaces for Face Recognition," in *Proc. Int. Conf. Biometrics*, pp. 424-433, Italy, 2009.
[14] U. Park and A.K. Jain, "Face Matching and Retrieval Using Soft Biometrics," *IEEE TIFS*, vol. 5, no. 3, pp. 406-415, 2010.
[15] N. Srinivas, G. Aggarwal, P.J. Flynn, and R.W.V. Bruegge, "Facial Marks as Biometric Signatures to Distinguish Between Identical Twins," in *Proc. CVPR Workshops*, pp. 106-113, Colorado Springs, 2011.
[16] The U.S. Attorney's Office, Central District of California, Release No. 08-074, "Ex-marine Guilty of Using Drugs and Force to Have Sex with Young Girls in Cambodia," 29 May 2008. Available: http://www.justice.gov/usao/cac/Pressroom/pr2008/074.html
[17] *United States v. Pepe*, Case No. 07-168-DSF. Trial transcript, May 5, 2008.
[18] A. Nurhudatiana, A.W.K. Kong, K. Matinpour, S.Y. Cho, and N. Craft, "Fundamental Statistics of Relatively Permanent Pigmented or Vascular Skin Marks for Criminal and Victim Identification," in *Proc. IJCB*, pp. 1-6, Washington DC, 2011.
[19] H.P. Soyer, G. Argenziano, R. Hofmann-Wellenhof, and R.H. Johr (Eds.), *Color Atlas of Melanocytic Lesions of the Skin*, Springer, 2007.
[20] K. Kane, J.B. Ryder, R.A. Johnson, H.P. Baden, and A. Stratigos, *Color Atlas & Synopsis of Pediatric Dermatology,* McGraw-Hill, 2002.
[21] J. L. Aguilar, "Melanocyte Nevus in Childhood," *An. Esp. Pediatr.,* vol. 54, no. 5, pp. 477-483, 2001.
[22] K.Y. Suh and J.L. Bolognia, "Signature Nevi," *J. Am. Acad. Dermatol.,* vol. 60, no. 3, pp. 508-514, 2009.
[23] J.M. Grichnik, A.R. Rhodes, and A.J. Sober, "Benign Neoplasias and Hyperplasias of Melanocytes," in *Fitzpatrick's Dermatology in General Medicine,* 7th ed., McGraw-Hill, 2008.
[24] W.D. James, T.G. Berger, and D.M. Elston, *Andrew's Diseases of the Skin: Clinical Dermatology,* 10th ed., Saunders, 2005.
[25] J. Chen and Y.S. Moon, "A Statistical Study on the Fingerprint Minutiae Distribution," in *Proc. IEEE ICASSP*, pp. II-169-II-172, Toulouse, France, 2006.
[26] S.L. Sclove, "The Occurrence of Fingerprint Characteristics as a Two Dimensional Process," *J. American Statistical Association*, vol. 74, no. 367, pp. 588-595, 1979.
[27] D.A. Stoney, "Distribution of Epidermal Ridge Minutiae," *American J. Physical Anthropology*, vol. 77, no. 3, pp. 367-376, 1988.
[28] S. Pankanti, S. Prabhakar, and A.K. Jain, "On the Individuality of Fingerprints," *IEEE TPAMI*, vol. 24, no. 8, pp. 1010-1025, 2002.
[29] J. Chen and Y.S. Moon, "A Minutiae-based Fingerprint Individuality Model," in *Proc. IEEE CVPR*, pp. 1-7, Minneapolis, 2007.
[30] J. Chen and Y.S. Moon, "The Statistical Modeling of Fingerprint Minutiae Distribution with Implications for Fingerprint Individuality Studies," in *Proc. IEEE CVPR*, pp. 1-7, Anchorage, 2008.
[31] D. Maltoni, D. Maio, A.K. Jain, S. Prabhakar, "Fingerprint Individuality," in *Handbook of Fingerprint Recognition*, New York: Springer, 2003.
[32] S.N. Srihari and H. Srinivasan, "Individuality of Fingerprints: Comparison of Models and Measurements," *Center of Excellence for Document Analysis and Recognition (CEDAR) Technical Report TR-02-07, Department of Computer Science and Engineering University at Buffalo,* 2007.
[33] Y. Zhu, S.C. Dass, and A.K. Jain, "Statistical Models for Assessing the Individuality of Fingerprints," *IEEE TIFS*, vol. 2, no. 3, pp. 391-401, 2007.

[34] Y. Chen and A. K. Jain, "Beyond Minutiae: A Fingerprint Individuality Model with Pattern, Ridge and Pore Features," in *Proc. Int. Conf. Biometrics*, pp.523-533, Italy, 2009.
[35] G. Fang, S. Srihari, and H. Srinivasan, "Generative Models for Fingerprint Individuality Using Ridge Types," in *Proc. Int. Symposium on Information Assurance and Security*, pp. 423-428, Manchester, 2007.
[36] C. Su and S. N. Srihari, "Generative Models for Fingerprint Individuality using Ridge Models," in *Proc. ICPR,* pp.1-4, Tampa, Florida, 2008.
[37] P.J. Diggle, *Statistical Analysis of Spatial Point Patterns*, London: Oxford University Press, 2003.
[38] O. Schabenberger and C.A. Gotway, *Statistical Methods for Spatial Data Analysis*, Chapman & Hall/CRC Press, 2005.
[39] J. Illian, A. Penttinen, H. Stoyan, and D. Stoyan, *Statistical Analysis and Modelling of Spatial Point Patterns*, Wiley-Interscience, 2008.
[40] J.F. Heltshe and T.A. Ritchey, "Spatial Pattern Detection Using Quadrat Samples," *Biometrics*, vol. 40, no.4, pp.877-885, 1984.
[41] G.T. Pack, N. Lenson, and D.M. Gerber, "Regional Distribution of Moles and Melanoma," *A.M.A. Arch. Surgery*, vol. 65, no. 6, pp. 862-870, 1952.
[42] G.T. Pack, J. Davis, and A. Oppenheim, "The Relation of Race and Complexion to the Incidence of Moles and Melanomas," *Ann. New York Acad. Sci.*, vol. 100, pp. 719-742, 1963.
[43] F.H. Rampen and P.E. de Wit, "Racial Differences in Mole Proneness," *Acta Dermato-Venerologica*, vol. 69, no. 3, pp. 234-236, 1968.
[44] M.G. Lewis and K. Johnson, "The Incidence and Distribution of Pigmented Naevi in Ugandan Africans," *British Journal of Dermatology*, vol. 80, no. 6, pp. 362-366, 1968.
[45] W.P. Coleman, L.E. Gately, A.B. Krementz, R.J. Reed, and E.T. Krementz, "Nevi, Lentigines, and Melanomas in Blacks," *Arch. Dermatology*, vol. 116, no. 5, pp. 548-551, 1980.
[46] Y.G. Kim and K.H. Cho, "Counts of Common and Atypical Melanocytic Nevi in Korean Young Men: Assessment of Their Risks and Correlations with Associated Factors," *J. Dermatology*, vol. 23, no. 5, pp. 315-319, 1996.
[47] S. Rokuhara, T. Saida, M. Oguchi, K. Matsumoto, S. Murase, and S. Oguchi, "Number of Acquired Melanocytic Nevi in Patients with Melanoma and Control Subjects in Japan: Nevus Count is a Significant Risk Factor for Nonacral Melanoma but not for Acral Melanoma," *J. Am. Acad. Dermatology*, vol. 50, no. 5, pp. 695-700, 2004.
[48] B. Zitova and J. Flusser, "Image Registration Methods: a Survey," *Image and Vision Computing*, vol. 21, no. 11, pp. 977-1000, 2003.
[49] A. Myronenko and X. Song, "Point Set Registration: Coherent Point Drift," *IEEE TPAMI*, vol. 32, no.12, pp. 2262-2275, 2010.
[50] I.E. Dror, C. Champod, G. Langenburg, D. Charlton, H. Hunt, and R. Rosenthal, "Cognitive Issues in Fingerprint Analysis: Inter- and Intra-expert Consistency and the Effect of a 'Target' Comparison, "*Forensic Science International*, vol. 208, pp. 10-17, 2011.
[51] D. Moreno-Ramirez, L. Ferrandiz, A. Nieto-Garcia, R. Carrasco, P. Moreno-Alvarez, R. Galdeano, E. Bidegain, J.J. Rios-Martin, and F.M. Camacho, "Store-and-forward Teledermatology in Skin Cancer Triage: Experience and Evaluation of 2009 Teleconsultations," *Archives of Dermatology*, vol. 143, no. 4, pp. 479-484, 2007.
[52] C.W. Heather, "Prison Inmates at Midyear 2009 – Statistical Tables," U.S. Bureau of Justice Statistics, June 2010. Available: http://bjs.ojp.usdoj.gov/content/pub/pdf/pim09st.pdf
[53] The Japan Times Online, "Record Number of Child Porn Arrests through June," 5 Aug 2011. Available: http://www.japantimes.co.jp/text/nn20110805a6.html
[54] Mirror News, "Mirror Special Investigation: Police Fear 60,000 Paedophiles are Sharing Vile Images," 16 Oct 2012. Available: http://www.mirror.co.uk/news/uk-news/police-fear-60000-paedophiles-are-sharing-1380937
[55] The Australian, "Customs Alarmed by Child Porn Rise," 7 Apr 2009. Available: http://www.theaustralian.com.au/news/customs-alarmed-by-child-porn-rise/story-e6frg6no-1225696957022
[56] A.K. Jain, R. Bolle, and S. Pankanti, *Biometrics: Personal Identification in Networked Society*, Kluwer Academic Publishers, 1999.
[57] ICE News Release, "HSI Seeks Public's Help Identifying 'Jane Doe' Producer of Child Pornography, Rescuing Young Child from Ongoing Sexual Abuse," 19 Dec 2012. Available: http://www.ice.gov/news/releases/1212/121219washingtondc.htm
[58] C. Tang, A.W.-K. Kong, and N. Craft, "Using a Knowledge-Based Approach to Remove Blocking Artifacts in Skin Images for Forensic Analysis," *IEEE TIFS*, vol. 6, no. 3-2, pp. 1038-1049, 2011.